Research Article

Tushar Gajjar, Dhaval B. Shah*, S. J. Joshi, and K. M. Patel

Experimental and simulation investigation on spring-in deformation for L-shape component

https://doi.org/10.1515/cls-2019-0014
Received Jul 01, 2019; accepted Aug 16, 2019

Abstract: The angular deformation is key parameter in composite manufacturing for curvature surfaces. Process Induced Distortions (PID's) are a major problem while manufacturing a composite part using autoclave process. Spring-back or spring-in is one of the PID in autoclave process. Spring-in effect either increase or decrease at angled section during curing of composite laminates. In this paper, L-shaped composite part has been manufactured using autoclave process. The material properties like glass transition temperature, heat reaction, crystallization temperature, Coefficient of Thermal Expansion have been measured for the cured component by using various testing techniques. Spring-in angle has been found for various number of layers and layup orientation. The simulation has been performed in ABAQUS software along with the COMPRO plug-in for each component. The variation of spring-in angle has been observed with changing material properties. The experimental results have been compared with simulation results. The percentage variation of spring-in deformation for experimental and simulation results has been found in the range of 5-7%.

Keywords: Spring-in deformation; Autoclave process; layup orientation; COMPRO

1 Introduction

A composite material is a combination of two or more chemically different materials on a macroscopic scale to get the best properties out of its constituents which are not possible to obtain from any other materials. A composite material widely used in space application, automobiles, etc. because of its extreme mechanical properties [1]. The curing process is the most crucial stage in the manufacturing of composite. The curing refers to the process of hardening of the polymer material by the cross-linking of the polymer chains [2]. There are many composite manufacturing techniques like hand layup process, autoclave process, vacuum infusion process and resin transfer moulding process etc. The autoclave process is mostly used for manufacturing a good dimensional accurate component [3]. Spring-in deformation is a major factor in curvature component. The value of spring-in deformation varies from different process to process [4]. The characterization of thermoset matrices for polymer composites requires the development of cure kinetic models to describe the state of cure within the polymer after the composite system has been subjected to a thermal history [5]. Many researchers worked on prediction of the spring-back deformation and warpage for the composite products using various processes. Shah *et al.* [6] investigated spring-back deformation using different layers, mould materials and lay-up orientation with single and double hold curing cycle in autoclave process. 3D scanning technique has been used for measuring spring back deformation. Tavakol *et al.* [7] studied mechanical properties like cure shrinkage, thermal strains, tool-part interface during cure. A square composite panel has been fabricated to validate the simulation results and obtain a pattern of distortion. The difference in CTE between the tool and the part has stimulated in the process-induced residual stresses and distortion in the parts causing the spring-in or spring-back. Bogetti and Gillespie [8] studied a relationship between complex gradient in temperature, degree of cure, process- induced residual stress and deformation using one dimensional cure simulation analysis with incremental laminated plate theory model. Johnston *et al.* [9] studied on the residual deformation model with heat transfer and resin cure and resin flow permits analysis of all major identified sources of process-induced deformation during the autoclave process. Model application demonstrated through prediction of process induced deformation of a number of variations of a simple L-shaped laminate. The model has been shown to provide accurate

***Corresponding Author: Dhaval B. Shah:** Mechanical Engineering Department, Institute of Technology, Nirma University, Ahmedabad 382 481, India; Email: dbshah@nirmauni.ac.in
Tushar Gajjar: Mechanical Engineering Department, Sardar Vallabhbhai National Institute of Technology, Surat 395 007, India
S. J. Joshi, K. M. Patel: Mechanical Engineering Department, Institute of Technology, Nirma University, Ahmedabad 382 481, India

predictions of both spring-back angle and warped shape of the final part. White and Hahn [10] introduced a Lam-Cure model comprising of cure kinetics and residual stress modules. The linear viscoelastic model used in the residual stress module and the thermal strain has taken to be significantly lower than the chemical shrinkage.

The properties of the cured component are very important and it depends on the selection of manufacturing processes. In autoclave process, the important properties after curing are glass transition temperature, heat reaction, crystallization temperature, Coefficient of Thermal Expansion etc. which can be measured by using various testing methods [11]. The temperature at which polymer changes from solid to softer material is called the glass transition temperature (T_g). The material became useless after reaching at temperate T_g [12]. Gracia-Fernández *et al.* [13] measured the dynamic T_g using Dynamic Mechanical Analysis (DMA) and temperature modulated using Differential scanning calorimetry (DSC). The correlation has been found by using quasi-isothermal conditions. Jonghyun Kim *et al.* [14] has studied on the cure kinetics of prepreg laminates by using dynamic and isothermal DSC techniques. Shim *et al.* [15] has performed the experiment by using different epoxy base prepreg for measurement of glass transition temperature. The dual temperature epoxy prepreg gave better characteristics compare to a commercial prepreg system in single curing time. Sbirrazzuoli *et al.* [16, 17] has performed experiments for isothermal and dynamic measurements of diglycidyl ether of bisphenol A (DGEBA) with m-phenylenediamine (m-PDA). The change in degree of cure and activation energy has been observed by using different methodology.

In this research paper, L-shape CFRP components have been manufactured by using autoclave process. The lay-up orientation and number of laminate have been selected as a process parameters. The spring-in angle has been measured for each component using universal bevel protector. The properties of material like glass transition temperature, heat of reaction and coefficient of thermal expansion have been measured for cured component. The spring-in angle has been simulated in ABAQUS software along with the COMPRO plug-in. The effect of each process parameters have been observed in simulation. The experimental results for spring-in angle have been compared with simulation results. The variation of spring-in angle with respect to changing the value of material properties has been studied.

2 Experimentation

2.1 Material selection

The aluminium AISI 6061 grade has been selected as a mould material due to better surface finish and easy machinability. The unidirectional Hinpreg HCU 200 has been selected as a prepreg material. The resin grade A45 has been taken as an epoxy. The mechanical properties for the prepreg are filament diameter 7μm, tensile strength of 4000 MPa, tensile modulus of 240 GPa, elongation 1.5%, filaments 12K. Similarly, mechanical properties for epoxy are tensile strength of 48MPa, tensile modulus of 2915 GPa, elongation 1.6%. Some excellent surface finished advance Hinpreg A45 prepreg has been taken for its suitable range of curing temperature and excellent mechanical properties [18, 19]. The universal bevel protector has been used for measurement of spring-in angle for manufactured component. The least count value of the universal bevel protector is 5”.

2.2 Manufacturing of CFRP L-shaped component

The aluminium AISI 6061 has been selected as a mould material. The vertical milling machine has been used for facing a mould. The final dimension of the machined mould was 72 mm × 72 mm × 250 mm. The final cut of 0.2 mm has been taken for the smooth surface finish. Similarly, the corner edge has been removed by applying 4 mm corner radius. The ball end mill tool has used for radial operation on a vertical milling machine. The corner angle is taken as 90°. The surface roughness has been measured by using Mitutoyo digital measurement tool named surface roughness tester. Three layers of release agent has been applied on the manufactured mould material because of easy removal of the component after curing. Hinpreg HCU200/A45 has been taken as carbon fiber prepreg material which was cut in L-shape and mounted on mould. Similarly, the prepreg layers have been applied accordingly. The entire mould has been kept in autoclave for curing as shown in Figure 1. The temperature of the autoclave has been maintained at 120°C for 60 minutes after that it closed the mould along with part has been removed after curing and the manufactured L-shaped CFRP component has been shown in Figure 2. The spring-in angle has been measured with universal bevel protector.

Similarly, four, eight, and twelve layer of laminate have been manufactured by using different orientation

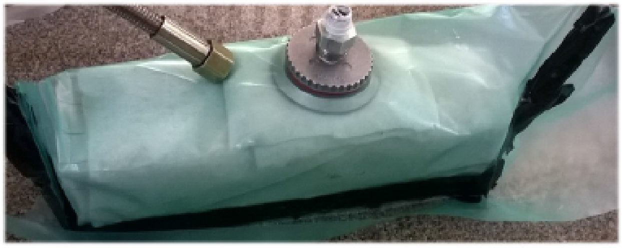

Figure 1: Mould along with part in autoclave oven

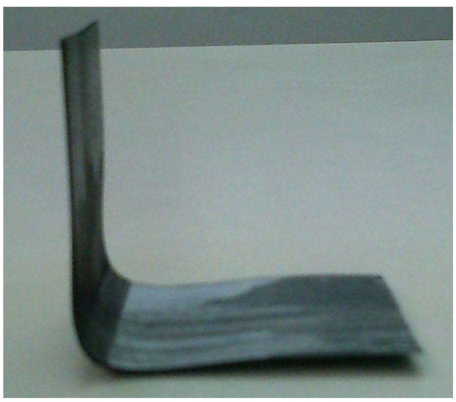

Figure 2: cured L-shaped component

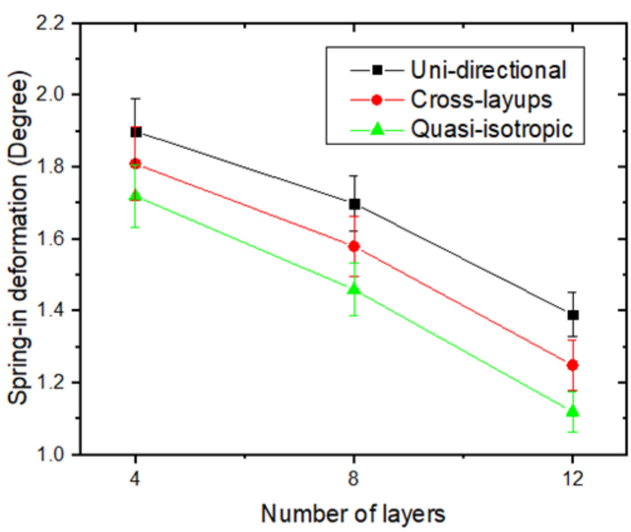

Figure 3: Spring-in angle deformation for different orientation with different layups

like uni-directional $[0]_S$, cross directional $[0/90]_S$ and quasi-isotropic $[0/45/-45/90]_S$. The spring-in angle has been measured by using universal bevel protector. The result of the spring-in angle for different orientations have been shown in Figure 3. It is observed that spring-in angle is minimum in quasi-isotropic direction. The uni-directional orientation gave maximum spring-in angle. Moreover, the spring-in deformation has been decreases with increasing number of layers.

The spring-in angle for each manufactured components have been simulated in ABAQUS software along with the COMPRO plug-in. There are many properties required as a input parameter and it also affecting on the final results so it is mandatory to find the value of different properties for the material. The Hexcel-8552/AS4 material is available in COMPRO library and the used material for the experiment is Hinpreg HCU200. So, the properties of material have been found using various testing experiments.

There are many processing parameters like the state of resin cure, glass transition temperature, cure shrinkage, thermal expansion, viscosity and stiffness which affects on spring-in deformation [5]. The properties covered under thermal analysis includes weight, dimension, dielectric constant, differential temperature etc. The primary thermal analysis techniques are: (i) Dynamic Mechanical Analysis (DMA), (ii) Differential Scanning Calorimetry (DSC), (iii) Thermo-Gravimetric Analysis (TGA), which are used for measuring a material properties. The thermal analysis techniques has been explained in following section for the Hinpreg HCU200/A45 material.

3 Material characterization

3.1 Dynamic Mechanical Analysis (DMA)

DMA is used for characterization of the material which mostly focus on the viscoelastic behaviour. The oscillating force or stress has been applied on the sample specimen and analyse the response of the material. The slope of stress and strain graph called as elastic modules which depends on temperature and applied stress. The elastic modules shows a working capacity of the material. The three point bending has been used in clamping arrangement for DMA analysis. It is more preferable for the stiff materials like carbon fibers. There are many factors affecting on the decreasing and increasing of the glass transition temperature like the flexibility of the main chain, branching, addition of plasticizers, increasing cohesive energy density, increasing molecular weight.

The test specimens have been cured in an autoclave at 160°C for three hours by using vacuum bagging techniques. The cured samples have been cut according to prescribed dimensions as per ASTM D7028 [21] using water jet cutting. Three point bending clamp has been attached to test specimen for the experiment as shown in Figure 4. The frequency of the setup was 1 Hz and heading rate

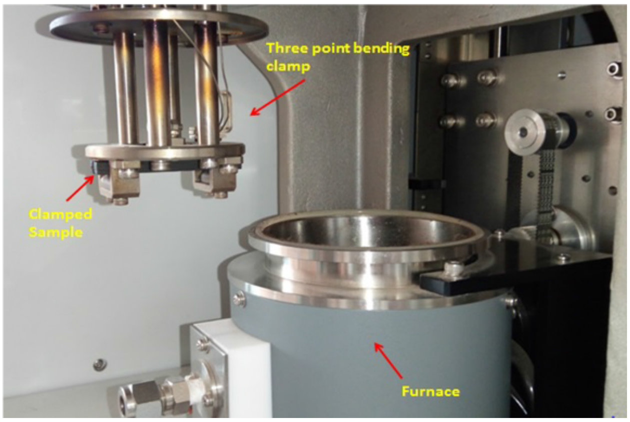

Figure 4: Three point clamping assembly

was 4°C/min. The temperature range has been taken between room temperature *i.e.* 34°C to 250°C. The Nitrogen has been taken as a purge flow gas for preventing contamination in the curing process.

The sinusoidal stress has been applied on the sample specimen with a frequency of 1 Hz. The corresponding strain has been measured using a linear variable differential transformer (LVDT). The graph of modulus v/s temperature along with the delta curve has been generated. The glass transition temperature has been determined for the cured sample according to ASTM D7028. The value of storage modulus, loss modulus and tan delta has been observed from the DMA test and the recorded results for test specimens have been plotted in ORIGIN software as shown in Figure 5. The glass transition temperature (T_g) has been obtained from the pick value of the tan delta curves.

3.2 Differential scanning calorimetry (DSC)

The DSC is a thermo-analytical technique in which amount of heat required is different with increase the temperature of the sample. The reference has been measured as the function of the temperature. The sample and reference have been maintained at approximately the same temperature in throughout he experiment [22]. The heat flow rate of the sample has been monitored against time as well as temperature while the temperature of the sample is programmed in specified atmosphere [23]. The dynamic scanning and isothermal scanning have been included in DSC scanning modes. The sample is heated at a constant heating rate in dynamic scanning while the sample has been kept at a constant temperature.

The ASTM D3418 standard has been followed for DSC testing. The weight of the sample was 3.627 mg. The ramp up time 50°C to 240°C with 10°C/min ramp up time. The

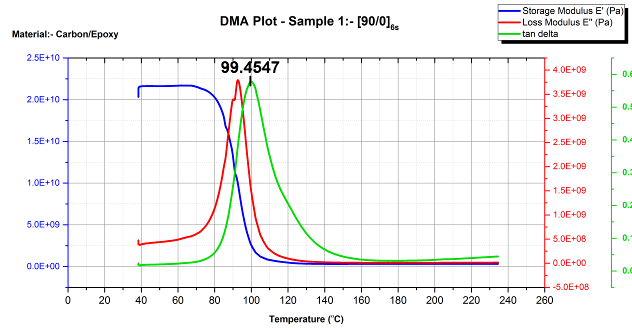

(a)

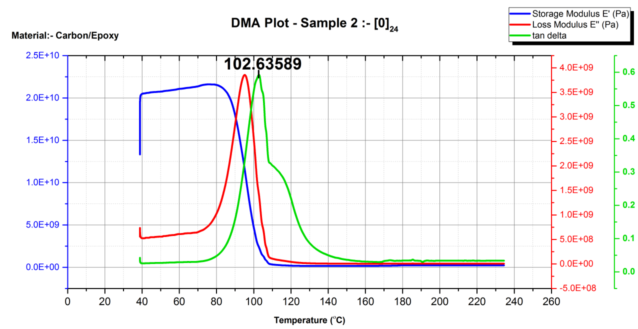

(b)

Figure 5: Glass transition temperature obtained using DMA test

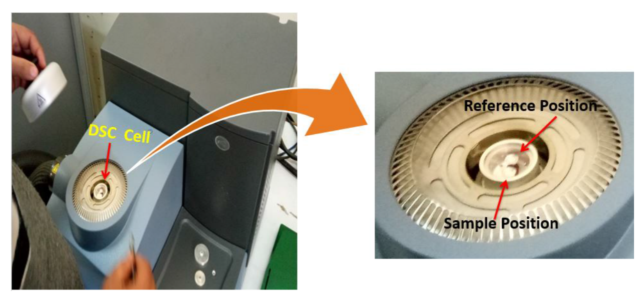

Figure 6: DSC cell with sample position

liquid has been poured in an aluminium pan and press for getting pan shape. The reference position is kept empty with just air as shown in Figure 6. The difference in heat flow between sample and reference has been measured. The nitrogen gas has been used for cooling in sample specimen placed in DSC cell.

The experimental data has been recorded in dynamic DSC mode from 50°C to 240°C at 10°C/min and plotted by using ORIGIN software as shown in Figure 7(a). The area of the curve is –56.37208 J/g which shows the heat of reaction (H_R). Similarly, the heat flow with respect to temperature has been shown in Figure 7(b). The peak value is 151.08°C which indicate the crystallization temperature. The glass transition temperature (T_g) has been taken from the intermediate point which equal to 108.61°C.

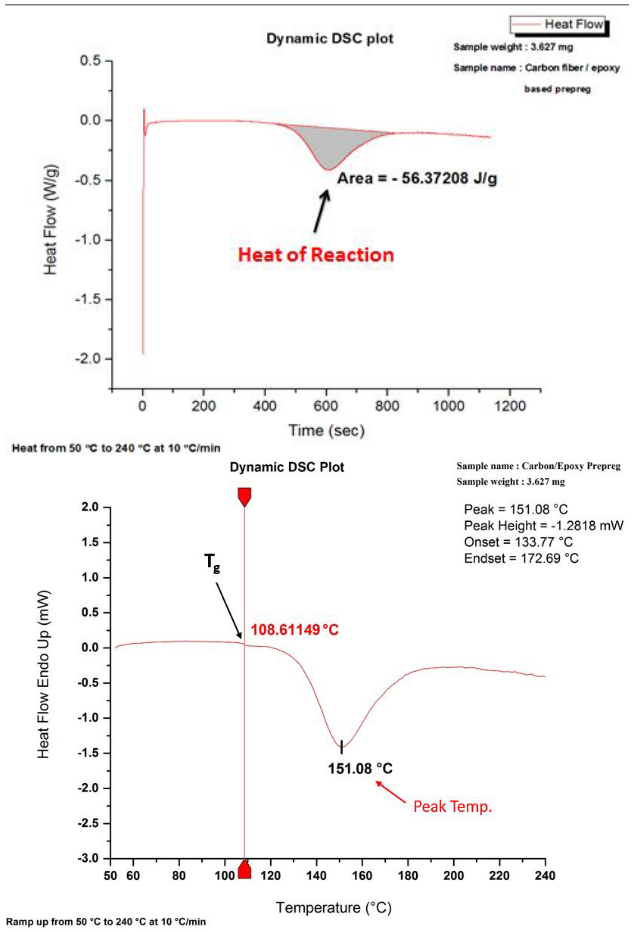

Figure 7: (a): Heat flow vs time in DSC test; (b): The glass transition temperature

3.3 Coefficient of Thermal Expansion (CTE) Measurement

CTE has been measured by changing the length per entire length of the material and temperature change in degree [7]. CTE is measured with following equation 1.

$$\text{CTE} = \alpha = \frac{(L_2 - L_1)}{[L_1(T_2 - T_1)]} \tag{1}$$

Where, L_1 and L_2 are the length of the specimen at temperature T_1 and T_2 respectively. CTE has determined the rate of the material expansion with the function of temperatures so the large value of the CTE represents the more sensitivity of the material with respect to change in temperature. The standard ASTM D696-08 testing method has been selected for getting linear thermal expansion with vitreous silica dilatometer. The temperature range has been taken between −30°C to 30°C [25]. The fused quartz-tube dilatometer used for this test. The change in temperature has been measured by using liquid bath and the change in temperature has been found by using device. The preconditioned specimen has been mounted into the dilatometer and entire assembly has been placed below to the liquid level of the bath. CTE has been determined according to equation 1. The sample specimen for the experiment has been taken as per DMA testing material. The value of CTE for cured CFRP laminate is 2.96×10^{-6} / K.

4 Simulation Approach

4.1 Modelling and methodology

ABAQUS CAE module has been used for making L-shape composite part with a bidirectional $[0/90]_{6s}$ configuration. The flange length of the L-shape part has been taken as 69 mm as shown in Figure 8. L-shaped part has been arranged with 24 plies. The thickness of each plies is 0.2 mm so the overall thickness of the L-shaped part is 4.8 mm.

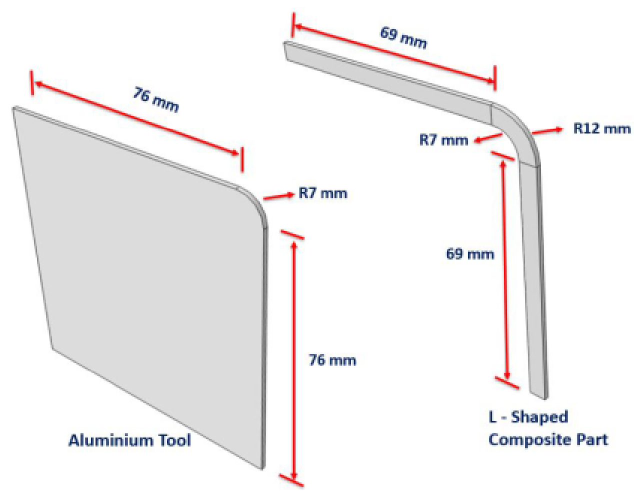

Figure 8: L-shaped composite part and aluminium tool

Cure kinetic parameters of Hexcel-8552/AS4 and Hinpreg-HCU200/A45 have been shown in Table 1 which is used for finding the effect of each cure kinetic parameter. The methodology has been decided with replacing a single cure kinetic material property one by one and at last change all properties at once while carrying out the simulation. Comparing simulated results with default material Hexcel-8552/AS4 as listed out in the COMPRO material database.

Table 1: Cure Kinetic Parameters of Hexcel-8552-AS4 and Hinpreg-HCU-200-A45

Parameter Name	Hexcel-8552-AS4	Hinpreg-HCU-200-A45
Heat of Reaction (J/kg)	5.4×10^5	-5.637×10^4
Pre-exponential Factor (1/s)	1.528×10^5	2.405×10^6
Activation Energy (J/mol)	6.650×10^4	9.194×10^4
CTE (1/K)	5.475×10^{-3}	2.96×10^{-6}

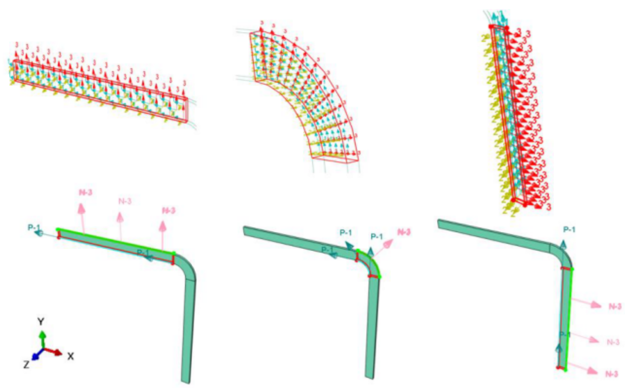

Figure 9: Material orientation assigned to the composite part

4.2 Material Assignment, Boundary Conditions and Meshing

Hexcel 8552/AS4 and Hinpreg HCU200/A45 prepreg system of composite laminated have been assigned in material selection. Similarly, mould material is assigned as Aluminium 6061 with solid homogeneous section. The stacking sequence for the composite part has been defined in solid as well as composite section. Material orientation has been assigned to different portions of the composite part in which three-direction have been kept in stacking direction. One-direction has been selected in the 0° fiber direction with the stacking direction for the curved portion in the part. The stacking direction kept along the thickness and 0° fiber direction along direction-1. The cylindrical coordinate system has been used with three-direction as the zero degree fiber direction. The material orientation for the composite part is as shown in Figure 9. where "N-3" shows the layer stacking direction and "P-1" shows the 0° fiber direction.

Mechanical displacement boundary conditions applied for constraining the composite and tool in space and at the same time expansion or contraction of the tool and part should be allowed during the whole process cycle.

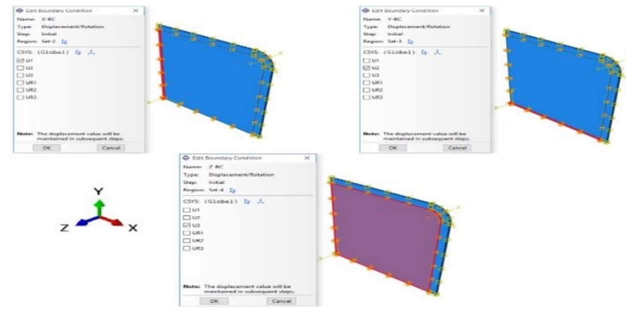

Figure 10: Displacement boundary conditions in X, Y and Z directions for global coordinate system

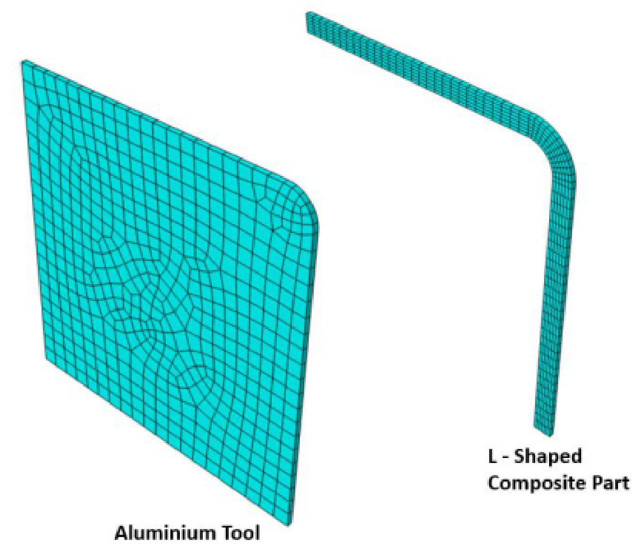

Figure 11: Meshed part and tool

This has accomplished by assigning the respective boundary condition to the surfaces of composite part and mould. The displacement boundary condition has been applied in the global coordinate system as well as local coordinate system as shown in Figure 10.

The mould-part interaction properties have been given by defining coefficient of friction as 0.15 and shear stress limit between composite and aluminium tool interface as 40000 N/mm^2. Initial boundary conditions like initial temperature and displacement has been given to respective surface. The meshing has been performed on mould and composite laminate. The quadratic C3D20 elements which can handle 3D stress have been used for the discretization process. The single element has been used to model individual layer across the thickness of the components. The composite part and mould have been meshed with 420 and 527 elements as shown in Figure 11.

Six layers across the thickness has been meshed in composite part as shown in Figure 12. Each element of single layers contains $[0/90]_S$ layup with thickness of 0.8 mm.

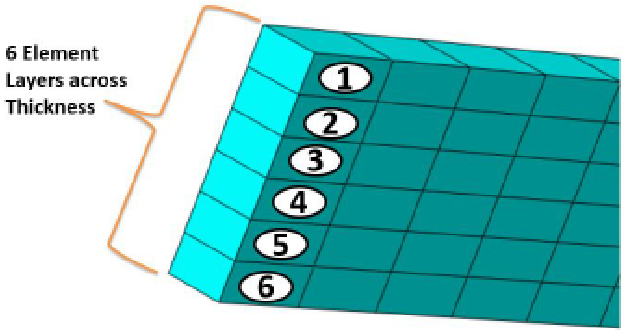

Figure 12: Number of elements across thickness in the composite part

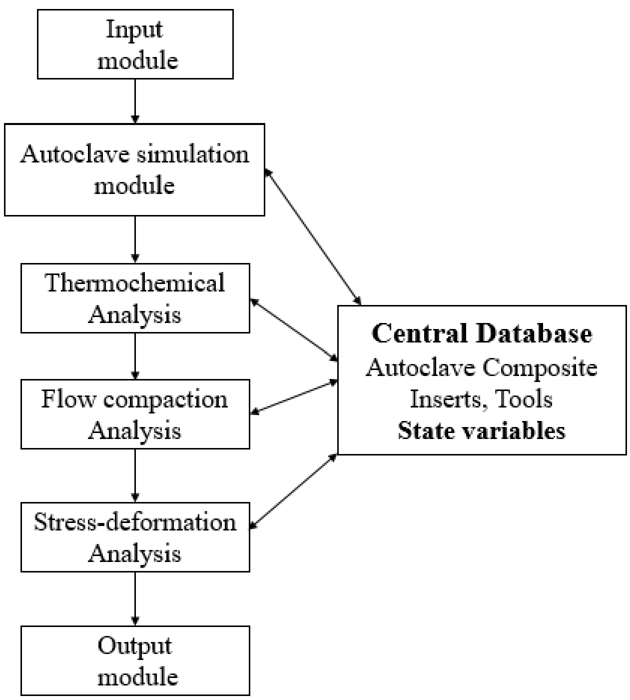

Figure 13: Line diagram of COMPRO structure and program flow

The stacking of all six elements made the layup as $[0/90]_{6s}$ and so, the total thickness of composite part become 4.8 mm. The individual parts has been separated after competing meshing.

4.3 Analysis Modules in COMPRO

COMPRO software has been used for getting spring-in deformation of L-shaped composite part. COMPRO carried three different analysis modules which are connected between each other as shown in Figure 13. The geometry of 3D model has been imported as an input module.

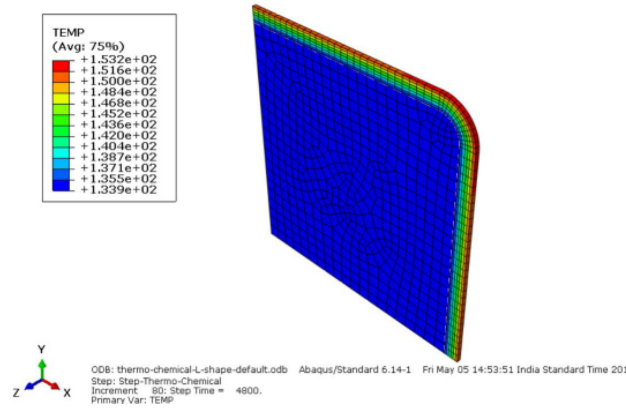

Figure 14: Thermochemical analysis

4.3.1 Thermochemical Analysis

Convective heat transfer boundary conditions have been applied to the top and bottom surfaces of the assembly while the edges have been assumed to be adiabatic means no heat transfer. The demonstration of thermal lag of the composite material and the mould material have been depended on the applied temperature cycle due to heat transfer condition. In addition, due to internal heat generation during cure, a temperature overshoot has been generated. The results of the analysis has also act as input to subsequent. Similarly, all steps have been followed by thermochemical analysis for getting stress deformation [26–29]. Thermochemical analysis took 24000 second in curing cycle. Heat transfer coefficient (HTC) has been defined at the top and bottom surface of assembly and it was 80 W/mK and 20 W/mK. Likewise, cure cycle has been also defined form of time and temperature amplitudes. The entire L-shaped composite part shown in Figure 14.

4.3.2 Flow-Compaction Analysis

The displacement boundary condition has been applied in the flow compaction analysis. Similarly, other boundary conditions like autoclave pressure and resin bleed also applied at the top surface of the composite part. This boundary conditions demonstrated the resin volume fraction, resin pressure gradients and thickness of the composite. The composite part thickness and fiber volume fraction distribution have been found at the end of the analysis. This results use as an input in the stress-deformation analysis [26]. Flow compaction step took 5100 second time for completing entire cycle. The complete flow-compaction analysis has been shown in Figure 15.

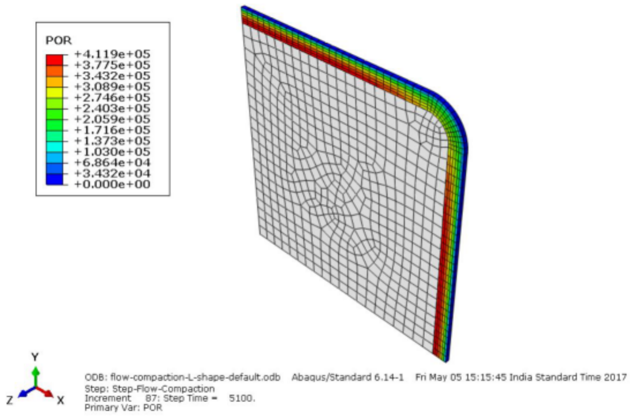

Figure 15: Flow compaction analysis

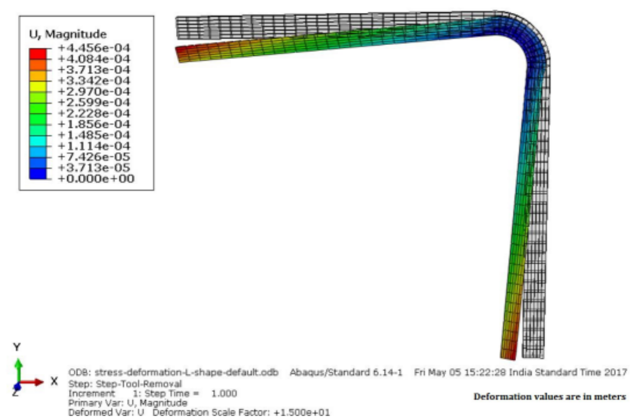

Figure 16: Stress deformation analysis

4.3.3 Stress-Deformation Analysis

The mould has been removed from the composite part and deform freely in stress-deformation module. The final deformed shape shows typical "spring-in" in the composite laminate [26] . These stress has been released after mould removal from the assembly and composite part resulting into spring-in. The spring-in shown in the simulation results as in Figure 16 was 15 times magnified than actual for better visualization.

4.4 Simulation Results

Hexcel 8552/AS4 material has been selected for the L-shape composite part. The entire process of simulation has been changed with respect to changing other permeates like heat of reaction, pre-exponential factor, activation of energy, CTE. Hinpreg HCU200/A45 material has been used for changing the parameters. Similarly, the spring-in value also change with these parameters. The final stress deformation analysis shown in the Figure 17.

Table 2: Spring-in Angles for L-shaped Part under Different Criterion

Criterion	Maximum Displacement (mm)	Spring-in Angle (Degree)
Hexcel-8552-AS4	0.4456	0.37
Changing Heat of Reaction	0.4453	0.3697
Changing Pre-exponential Factor	0.487	0.404
Changing Activation Energy	0.0192	0.0159
Changing CTE	0.01921	0.0159
Changing All	0.01921	0.0159

Similarly, Hexcel 8552/AS4 material replaced with Hinpreg HCU200/A45 for changing all the parameters. The stress-deformation analysis of the Hinpreg HCU200/A45 material has been shown in Figure 18.

4.5 Calculating Spring-in Angle in the L-shaped Part

The spring-in angle in the L-shaped composite part has been calculated as per the Equation 2.

$$\text{Spring-in angle} = \tan^{-1}(\text{max .displacement of flange / flange length}) \tag{2}$$

Spring-in angle measured after changing every parameters. Generated result has been listed out in Table 2. The changing activation energy highly effect on displacement and spring-in angle compared with heat of reaction, exponential factor and CTE.

4.6 Result and Discussion

The entire experiment has been carried out by considering different process parameters like layup orientation and number of laminates. This experimental work has been simulated in ABAQUS software along with the COMPRO plug-in. The experimental result of Hinpreg material has been compared with simulated results for unidirectional, cross and quasi-isotropic layup orientation as shown in Figure 19. The values getting form the simulation is higher than experimental results. The spring-in angle de-

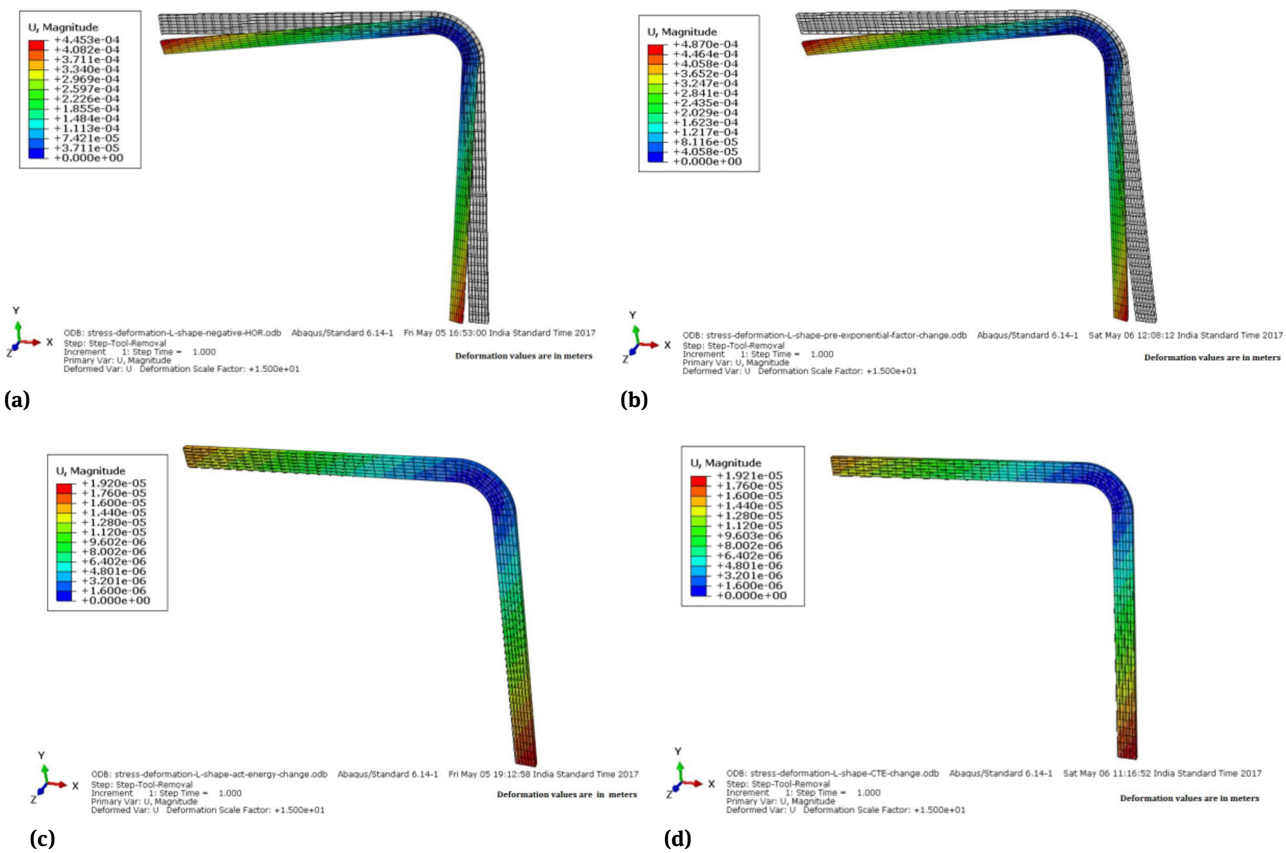

Figure 17: Stress deformation analysis after changing (a) heat reaction (b) Pre-exponential factor (c) activation of energy (d) CTE

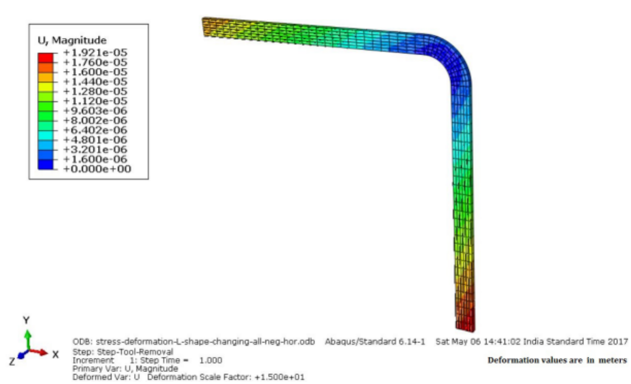

Figure 18: Stress deformation analysis of Hinpreg-HCU-200-A45 Material

viation for uni-directional sequence is near about 2° while spring-in angle deviation quasi-isotropic sequence is approximately 1.25°. The cross-layups orientation has fluctuated between 1.5° to 1.75°. The atmospheric temperature is never remain constant until finish the experiment so that result variation has been observed. The percentage error between experimental and simulation results is 5 to 7%. Moreover, the spring-in angle has been decreases with increasing number of layers.

The simulated results of Hinpreg and Hexcel material have been shown in Figure 20. The simulation has been performed for uni-directional, cross-layup and quasi-isotropic orientation. The Hexcel material have a high spring-in deformation with respect to Hinpreg. The high fluctuation has been found in quasi-isotropic layups. The spring-in deformation for 4 layers has been approximately 2° for both material in every orientation.

The experimental and simulated results of Hinpreg material compared with Hexcel material for 4, 8, 12 layers as shown in Figure 21. The simulated result of spring-in deformation for Hexcel material is much higher the Hinpreg results in every layers. The high variation found in cross layups compared to uni-directional and quasi-isotropic layups orientation.

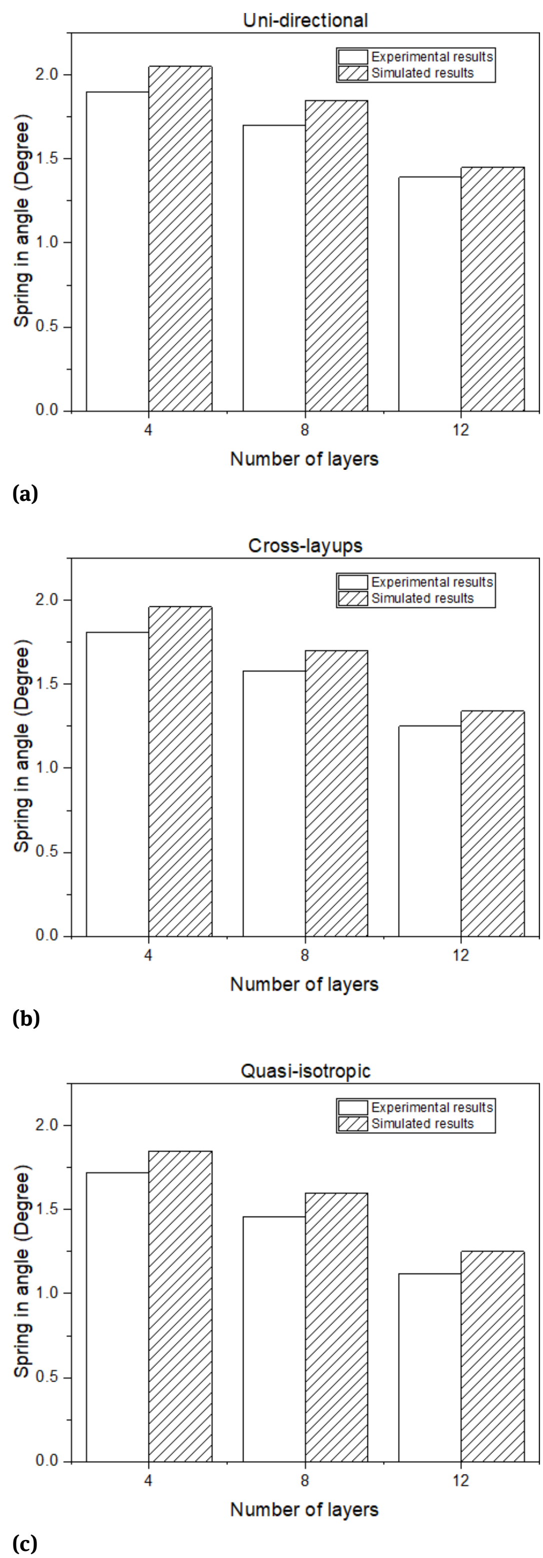

Figure 19: Comparison of experimental and simulation results of Hinpreg material for (a) uni-directional (b) cross-layup and (c) quasi-isotropic orientation

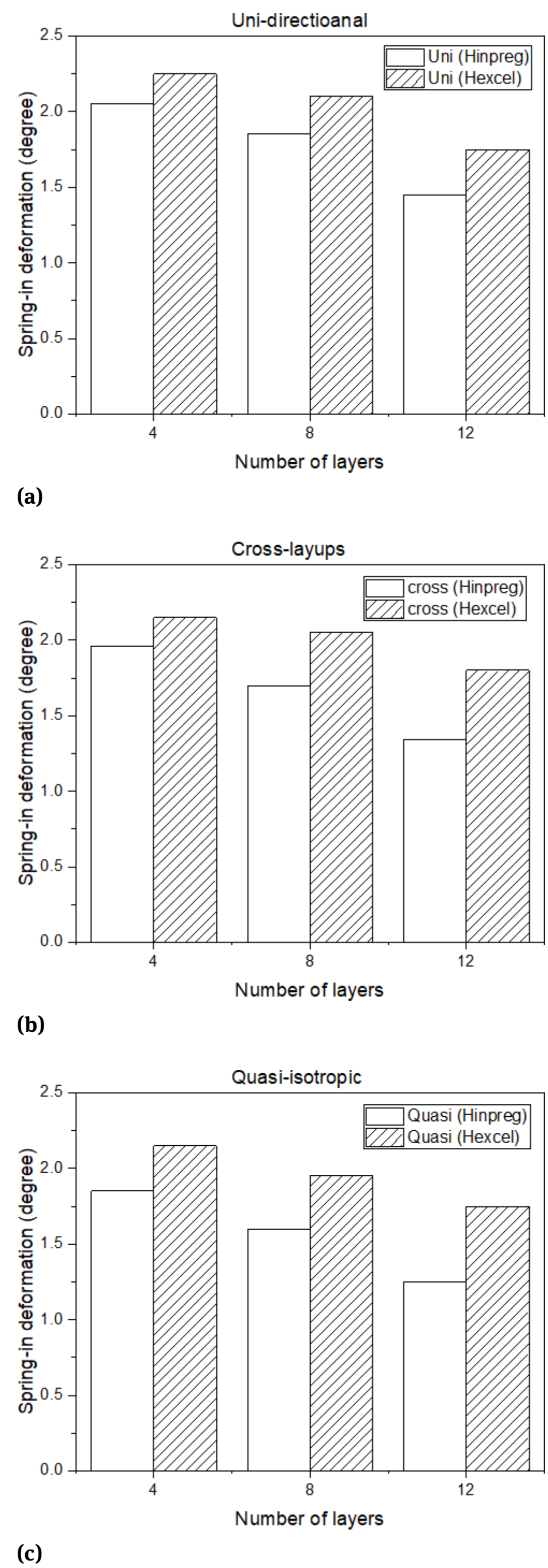

Figure 20: Simulated results compared for Hinpreg and Hexcel material for (a) uni-directional (b) cross-layup and (c) quasi-isotropic orientation

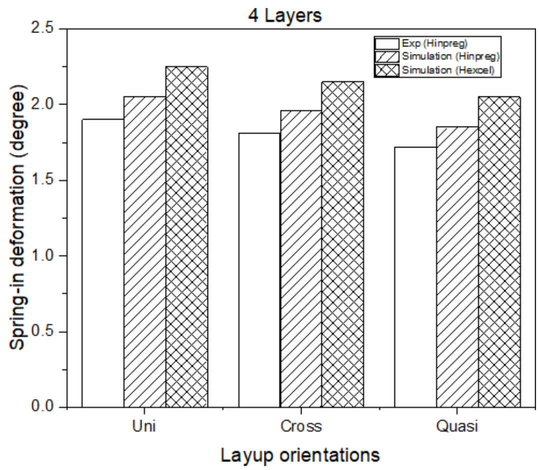

(a)

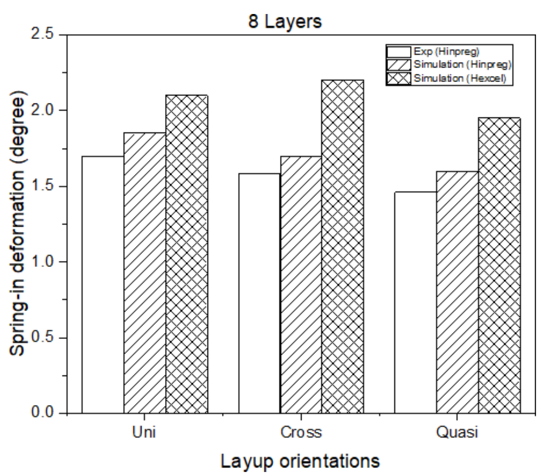

(b)

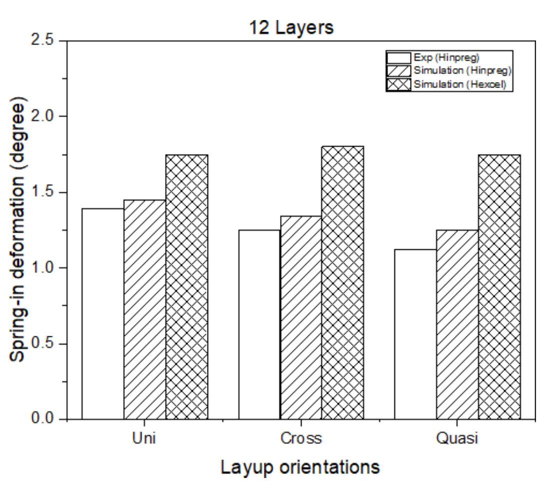

(c)

Figure 21: The experimental and simulated result of Hinpreg material compared with simulated results of Hexcel material for (a) 4 layers (b) 8 layers and (c) 12 Layers

5 Conclusion

The L-shape CFRP component has been manufactured by using autoclave manufacturing process. The aluminium AISI 6061 has been taken as a mould materials for experiment which machined by using vertical milling machining. The process parameters like layup orientation, number of laminate has been considered as a process parameters. The spring-in angle has been measured for each manufactured component by using Mitutoyo digital measurement tool. The quasi-isotropic sequence has a very less spring-in angle compare to uni-directional and cross directional layup orientation. The spring-in angle has been decreases with increasing number of laminates. The properties of cured component like glass transition temperature, heat of reaction and coefficient of thermal expansion have been measured by using analysis techniques. This properties used for input values during simulation. The ABAQUS software along with the COMPRO plug-in has been selected for simulation. The experimental result and simulated results have been compared for each cases. The experimental and simulated result of Hinpreg material compared with simulated results of Hexcel material for 4, 8, 12, number of layers and different layup orientation. The simulated result of spring-in deformation for Hexcel material is much higher the Hinpreg results in every layers. Similarly, the simulated results of Hinpreg material is also higher than experimental results in each layers as well as different layup orientation.

References

[1] I. M. Daniel and O. Ishai, Engineering mechanics of composite materials, 2nd ed. New York: Oxford University Press, 2006.
[2] Mazumdar S. K, Composites Manufacturing Materials, Product, and Process Engineering, CRC Press.
[3] Autar K. Kaw. Mechanics of Composite Materials. Taylor & Francis Group, LLC. CRC Press; 2006.
[4] Gajjar, Tushar., *et al.* "Prediction of Spring-back Deformation for CFRP Reflectors Manufactured using Various Processes." Journal of Applied Engineering Research Volume 13, Number 6 (2018) pp. 144-148
[5] L. A. Carlsson, D. F. Adams, and R. B. Pipes, Experimental characterization of advanced composite materials, 4. ed. Boca Raton, Fla.: CRC Press, 2014.
[6] Shah, Dhaval B., *et al.* "Experimental investigation on spring-back deformation during autoclave curing of parabolic antenna reflectors." Composites Part A: Applied Science and Manufacturing 115 (2018): 134-146.
[7] B. Tavakol *et al.*, "Prediction of residual stresses and distortion in carbon fiber-epoxy composite parts due to curing process using finite element analysis," Journal of Applied Polymer Science, vol.

128, no. 2, pp. 941–950, Apr. 2013
[8] T. A. Bogetti and J. W. Gillespie, "Process-Induced Stress and Deformation in Thick-Section Thermoset Composite Laminates," Journal of Composite Materials, vol. 26, no. 5, pp. 626–660, Jan. 1992
[9] A. Johnston, R. Vaziri, and A. Poursartip, "A Plane Strain Model for Process-Induced Deformation of Laminated Composite Structures," Journal of Composite Materials, vol. 35, no. 16, pp. 1435–1469, Jan. 2001
[10] S. R. White and H. T. Hahn, "Process Modeling of Composite Materials: Residual Stress Development during Cure. Part II. Experimental Validation," Journal of Composite Materials, vol. 26, no. 16, pp. 2423–2453, Jan. 1992
[11] Hardis, Ricky, Cure kinetics characterization and monitoring of an epoxy resin for thick composite structures" (2012). Graduate Theses and Dissertations. Paper 12608.
[12] V. Shah, Handbook of plastics testing technology. New York: Wiley, 1984.
[13] Gracia-Fernández, C. A., Gómez-Barreiro, S., López-Beceiro, J., Saavedra, J. T., Naya, S., & Artiaga, R. (2010). Comparative study of the dynamic glass transition temperature by DMA and TMDSC. Polymer Testing, 29(8), 1002-1006.
[14] J. Kim, T. J. Moon, and J. R. Howell, Cure Kinetic Model, Heat of Reaction, and Glass Transition Temperature of AS4/3501-6 Graphite-Epoxy Prepregs," Journal of Composite Materials, vol. 36, no. 21, pp. 2479-2498, Nov. 2002.
[15] Shim, S. B., Seferis, J. C., Eom, Y. S., & Shim, Y. T. (1997). Thermal characterization and comparison of structural prepregs with different cure temperatures. Thermochimica Acta, 291(1-2), 73-79.
[16] Sbirrazzuoli, N., Vyazovkin, S., Mititelu, A., Sladic, C., & Vincent, L. (2003). A study of epoxy-amine cure kinetics by combining isoconversional analysis with temperature modulated DSC and dynamic rheometry. Macromolecular Chemistry and Physics, 204(15), 1815-1821.
[17] Vyazovkin, S., & Sbirrazzuoli, N. (1996). Mechanism and kinetics of epoxy- amine cure studied by differential scanning calorimetry. Macromolecules, 29(6), 1867-1873.
[18] Hindoostan Composite Solution Technical Data Sheet Manual.
[19] HexPly® Prepreg Technology Manual.
[20] K. P. Menard, Dynamic mechanical analysis: a practical introduction. BocaRaton, Fla: CRC Press, 1999.
[21] S. R. Sandler, Ed., Polymer synthesis and characterization: a laboratory manual. San Diego: Academic Press, 1998.
[22] S. K. Nayak, S. N. Yadav, and S. Mohanty, Fundamentals of plastic testing. Spinger Publications, 2012.
[23] G.Hohne, W. Hemminger, and H.-J. Flammersheim, Differential scanning calorimetry: an introduction for practitioners. Berlin; New York: Springer-Verlag, 1996.
[24] Lee, W. I., Loos, A. C., & Springer, G. S. (1982). Heat of reaction, degree of cure, and viscosity of Hercules 3501-6 resin. Journal of Composite Materials, 16(6), 510-520.
[25] ASTM (2003) D696: Standard Test Method for Coeffcient of Linear Thermal Expansion of Plastics Between −30°C and 30°C with a Vitreous Silica Dilatometer. ASTM International, West Conshohocken, PA, USA.
[26] Compro Corner Section Examples, Convergent Manufacturing Technologies Inc. (2014).
[27] COMPRO for ABAQUS Modeling Guidelines, Convergent Manufacturing Technologies Inc. (2016).
[28] Compro Model Documentation, Release 1.5.8, Convergent Manufacturing Technologies Inc. (2017).
[29] Abaqus 14.1 Manual.